

FERA: Bridging the Semantic Gap in Foil Fencing via Kinematic Pose Recognition and Explainable Rule Reasoning

Ziwen Chen
 Marc Garneau Collegiate Institute (TDSB)
 Toronto, Canada
 ziw08@gmail.com

Zhong Wang
 Dalian University of Technology (DUT)
 Dalian, China
 zhongwang@dlut.edu.cn

Abstract

Foil fencing presents a unique multimedia challenge: actions are extremely fast, interactions are subtle, and the final right-of-way decision relies on complex linguistic rules applied to visual data. We present FERA (Fencing Referee Assistant), a pose-based framework that bridges the gap between pixel-level perception and semantic rule reasoning. From monocular video, FERA extracts 2D poses, converts them into a compact 101-dimensional kinematic representation, and applies an encoder-only Transformer (FERA-MDT) to predict multi-label footwork and blade actions. Crucially, these predictions serve as semantic tokens for a downstream language model (FERA-LM) to generate explainable verdicts. Training treats left and right fencers symmetrically by creating two single-fencer sequences per clip. At inference, FERA-MDT uses dynamic temporal windowing to handle variable-length clips, and paired predictions are passed to FERA-LM, which applies encoded right-of-way rules to generate prototype decisions and short explanations. On 1,734 clips (2,386 move instances) from professional bouts, FERA-MDT reaches a macro-F1 of 0.549 under 5-fold cross-validation, outperforming a BiLSTM, TCN, and baseline Transformer. Furthermore, we demonstrate that our structured outputs enable a language model to perform logical rule reasoning, effectively decoupling visual perception from rule application. FERA provides the first dataset and benchmark for this cross-modal action understanding task.

1. Introduction

In fencing, referees must evaluate blade interactions, interpret right-of-way, and determine who initiated or interrupted the attack at high speed. Even at official competitions, disputes arise; in clubs, bouts are often refereed by fellow members or proceed without a referee at all.

Automated assistance in fencing is not merely a com-

puter vision problem; it is a multimodal translation challenge. The system must bridge the semantic gap: translating raw high-speed video pixels into geometric pose data, then into discrete semantic actions (e.g., *Parry*, *Lunge*), and finally into a linguistic explanation of the rule outcome. While electronic scoring systems indicate *when* a touch occurs, they cannot explain *why* a point was awarded.

Problem definition. Given a short monocular video clip (approximately 1–3 seconds) centered on a foil exchange, the goal is to:

1. track both fencers,
2. for each fencer, predict a set of footwork and blade actions (multi-label) and a single blade-line position, and
3. consume these per-fencer predictions in a reasoning module that outputs a right-of-way decision and short explanation.

This separates perception (pose-based multi-label action and blade recognition) from reasoning (mapping paired move sequences to referee decisions), allowing each to be evaluated and improved independently.

In our experiments we adopt a trimmed-clip setting for supervised training and cross-validation, where each example corresponds to a manually labeled single-fencer exchange. At inference on longer or untrimmed bout streams, we instead run FERA-MDT with a dynamic temporal windowing scheme over per-fencer pose tracks, so the model does not assume that exchange boundaries or move start/end frames are known in advance.

To support this task, we created a new dataset and labeling protocol. Each clip is drawn from a professional bout and assigned a unique identifier. For recognition, we adopt a canonical single-fencer view: the model always sees a fencer on the left side of the piste. Practically, we annotate the left fencer in the original video, then create a horizontally flipped version of the clip and annotate the original right fencer, who now appears on the left. This yields up to two single-fencer sequences per exchange (one per side),

linked by the same clip ID, and lets FERA-MDT train on one skeleton at a time while learning from both fencers.

FERA framework. FERA (**FE**ncing **RE**feree **A**ssistant) is a four-stage pipeline:

1. extract 2D poses for both fencers from monocular video,
2. compute kinematic and temporal features from each fencer’s pose sequence,
3. apply an encoder-only Transformer for per-fencer multi-label move and blade classification (FERA-MDT), and
4. consume paired left/right predictions in a distilled language model that applies encoded right-of-way rules (FERA-LM).

FERA is trained and evaluated on our dataset, the FERA-Dataset. In this paper we focus on the motion recognition and calibration aspects of FERA-MDT and provide a qualitative demonstration of language-based reasoning. The dynamic temporal windowing stage allows the same model trained on trimmed single-fencer segments to be deployed on arbitrary-length per-fencer pose tracks.

Contributions. This paper:

- introduces the FERA-Dataset, a foil fencing benchmark built from two-fencer exchanges, with frame-level annotations of footwork, blade actions, and blade-line positions represented as single-fencer sequences in a canonical left-facing view,
- proposes FERA-MDT, an encoder-only Transformer for pose-based multi-label move and blade recognition, with analysis of calibration and error patterns against strong baselines (BiLSTM, TCN, and a vanilla Transformer),
- demonstrates a decoupled vision-to-language reasoning pipeline (FERA-LM), showing that structured action recognition outputs can serve as semantic tokens for rule-based explanation generation, and
- releases annotations, derived pose features, and baseline code to support research on pose-based motion understanding and AI-assisted sports officiating.

2. Related Work

2.1. AI in fencing

FenceNet and related models report over 85% accuracy on the Fencing Footwork Dataset [17, 28], which contains 652 videos from 10 fencers annotated with footwork actions such as step forward, step backward, and several lunge variants. While useful for footwork modeling, the dataset omits blade actions that are essential for foil refereeing and uses a single recording environment with fixed, straight-on angles. Each video shows only one fencer, without opponent exchanges or reflexive responses.

These conditions simplify training and boost reported accuracy but do not reflect full bouts with two interact-

ing fencers, diverse speeds, and varied camera perspectives. Our dataset and labeling protocol address these limitations by (i) accounting for two interacting fencers, (ii) including both footwork and blade actions, and (iii) using real competition footage with varied viewpoints, at the cost of increased modeling difficulty.

2.2. Pose estimation and tracking

Human pose estimation converts raw video into structured joint representations for downstream analysis. OpenPose introduced Part Affinity Fields to detect body parts and group them into individuals [4]. Later top-down methods improved accuracy by cropping per-person bounding boxes before extraction [25], and vision transformers such as ViTPose further improved accuracy through large-scale pre-training [26]. We use MMPose [18] with RTMPose [12] for pose estimation and RTMDet [16] for bounding box detection; RTMPose is lightweight and real-time while maintaining competitive accuracy.

Tracking identities and poses over time, especially under occlusions or when fencers cross paths, is challenging. Multi-object trackers such as DeepSORT [23] and ByteTrack [27] link detections over time, with ByteTrack retaining low-confidence detections to avoid losing objects during fast, blurry frames. FERA instead uses a custom tracker tailored for fencing, combining a distance function with Norfair [21, 22] to maintain two consistent fencer tracks per clip.

2.3. AI-assisted refereeing in sports

Beyond fencing, AI-assisted refereeing and explainable decision systems have been explored in sports such as soccer. Recent work on Video Assistant Referee Systems (VARs) develops multi-view pipelines for foul detection and off-side decisions and uses large language models for human-interpretable explanations [6, 9, 10]. Benchmarks such as SoccerNet explicitly target temporal localization of fouls, multi-modal reasoning, and explanation quality in realistic broadcast footage.

FERA extends this line of work to foil fencing, where exchanges are shorter, motion is faster and more linear, and right-of-way depends on subtle blade timing rather than continuous physical contact. We focus on pose-based single-fencer action recognition and its calibration; language-based reasoning over recognized actions builds directly on recent VARs-style approaches.

3. FERA-Dataset

We constructed the FERA-Dataset to capture realistic two-fencer exchanges under varied camera angles. It is derived from professional match videos (720p, 25 fps) from three Grand Prix competitions involving approximately 130 competitors. Each match video is segmented into the final seven

seconds preceding a touch. Referee decisions are inferred by analyzing the score: if the score changes before another touch occurs, a point is awarded. Aligning score changes with detected hit events yields clips paired with referee outcomes for the rule-reasoning subset. Each clip is then manually annotated to identify the moves performed by each fencer.

3.1. Dataset specifics and labeling

Many fencing videos display static overlays for scoring and hit lights. We manually locate the hit-light and score regions and compare reference images to video frames; if the color similarity exceeds tuned thresholds, a hit is detected, and digit recognition recovers the score. These signals are used only to align clips with referee decisions; all move and blade annotations are manual.

Actions are annotated frame by frame using a custom interface (Figure 1). Each clip has a unique identifier. We adopt a canonical view in which the fencer of interest always appears on the left:

- In the original clip, annotators label the fencer on the left side of the piste.
- In a flipped view, the clip is mirrored horizontally and annotators label the original right fencer, now on the left.

In both passes, the labeling scheme is identical. For the visible (left) fencer, each continuous segment is assigned one or more of:

step forward, step backward, half step forward, half step backward, lunge, flèche, wait, parry, beat, counterattack, fake, hit

and one blade position from {4, 6, 7, 8, other}. In cases where moves overlap (e.g., beat + step forward), the interval is marked by the endpoints of the longer action, and both labels are retained.

Note to fencers: the *hit* label indicates that the fencer extended their arm with the intention to score and does not guarantee that contact was successful.



Figure 1. Custom labeler for per-fencer moves and blade positions. Visualized pose estimates help identify labeling or tracking failures; clips with unreliable fencer selection are discarded.

Each annotated example can be viewed as a single-fencer sequence of time-stamped records:

$$\{(t_k, \mathcal{Y}_k, b_k)\}_{k=1}^K,$$

where $\mathcal{Y}_k \subseteq \{1, \dots, 12\}$ is the set of active move labels for the (left-view) fencer at interval k , and $b_k \in \{4, 6, 7, 8, \text{other}\}$ is the corresponding blade position. When both sides are annotated, a clip with identifier c yields two sequences, (c, left) and (c, right) , which share the same time axis but are stored and trained as separate single-fencer examples.

FERA-MDT is trained purely on these single-fencer sequences in the canonical left view. At inference, we extract pose tracks for each fencer, mirror the right-side track if needed, apply FERA-MDT independently using dynamic temporal windowing (Section 4), and then realign the resulting move and blade sequences on the shared time axis before passing them to FERA-LM.

3.2. Data distribution

We use 1,734 clips and 2,386 annotated move instances across all single-fencer sequences. On average, each clip contains 1.38 moves. The moves are skewed, with step forward (28.8%), hit (19.9%), and step backward (14.6%) most common, while rare moves such as flèche account for less than 1% (Table 1a).

Table 1. Dataset distributions for moves and blade positions.

(a) Moves			(b) Blade positions		
Move	Count	%	Blade position	Count	%
Step forward (1)	687	28.8	6	1114	64.2
Step backward (2)	349	14.6	8	410	23.6
Half step forward (3)	127	5.3	7	95	5.5
Half step backward (4)	87	3.6	4	85	4.9
Lunge (5)	232	9.7	Other	30	1.7
Flèche (6)	11	0.5			
Wait (7)	71	3.0			
Parry (8)	72	3.0			
Beat (9)	150	6.3			
Counterattack (10)	77	3.2			
Fake (11)	49	2.1			
Hit (12)	474	19.9			

Blade positions are highly imbalanced: position 6 accounts for 64.2% of annotations, followed by 8 (23.6%), while 4, 7, and other together represent 12.2%. This reflects typical foil tactics, where most fencers rely on one or two blade lines, making rare move/blade combinations extremely uncommon.

Data ethics and availability. All source videos are publicly available competition recordings. We work only with broadcast footage and do not collect additional identifying information. All annotations were created manually by fencing experts. Released data are anonymized and consist of derived pose sequences and labels. We provide a

research-access package containing pose sequences, kinematic features, annotations, and training/evaluation code for all baselines; the project page URL is in the supplementary material.

Task formulation. We adopt a trimmed-clip recognition setup for training and evaluation: each example is a short clip centered on an exchange, and the goal is to predict the set of moves and blade position active in that interval for a single fencer. In the deployed pipeline, however, we run FERA-MDT with the dynamic temporal windowing scheme described in Section 4 on arbitrary-length per-fencer pose sequences extracted from bout footage, so clip-level exchange boundaries are not required at test time. Extending FERA to fully annotated action spotting on untrimmed broadcasts—localizing and classifying all actions over entire bouts and evaluating them directly—remains important future work.

4. Methodology

4.1. FERA pipeline overview

The FERA pipeline converts raw video into structured referee inputs and, optionally, decisions through four stages: (i) pose estimation, (ii) feature engineering, (iii) Transformer-based move and blade detection (FERA-MDT), and (iv) language-model reasoning (FERA-LM). FERA operates on one fencer at a time during recognition. For each clip or longer bout segment, pose and feature sequences for the left and right fencers are extracted separately, processed by a shared FERA-MDT model with dynamic temporal windowing, and decoded into per-fencer move sequences and blade positions. Predictions are then aligned on the shared time axis, combined with encoded priority rules, and optionally passed to FERA-LM. Dynamic temporal windowing bridges the gap between training on trimmed single-fencer examples and inference on continuous per-fencer pose streams.

4.2. Pose estimation

The first stage of FERA identifies the two active fencers and tracks their skeletons across frames, under occlusion and motion. This stage includes fencer filtering, tracking, and joint extraction.

Fencer filtering. At the start of each clip, we search for candidate fencers during a short grace period. Candidates must occupy at least 3% of the frame area, exceed a confidence threshold (> 0.20), and not touch the bottom edge (referees are often visible only from the torso upward). Each candidate is scored by size and vertical placement to prioritize likely fencers.

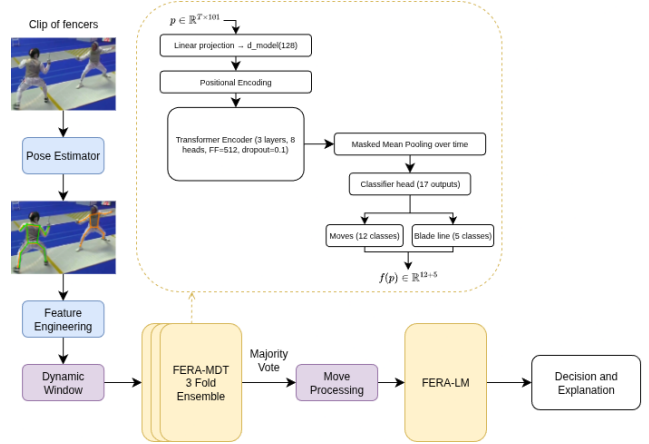


Figure 2. FERA pipeline: pose estimation, feature engineering, move/blade detection (FERA-MDT), and rule reasoning (FERA-LM).

Tracking. Tracking uses Norfair with a custom distance function combining intersection-over-union (IoU) and centroid distance [21, 22]. If an ID is lost, the system reassigns it by matching new detections to the last known bounding box via IoU, with pose similarity scoring to prevent switches to background individuals. A light exponential moving average (EMA) smooths joint trajectories, retaining valid positions when detections are missing and reducing jitter.

Pose extraction. Bounding boxes and skeletons are obtained using MMDetection and MMPose [5, 18]. We employ `rtmpose-m_8xb256-420e_coco-256x192` for pose extraction and `rtmdet_tiny_8xb32-300e_coco` for detection, chosen as fast RTMPose [12] and RTMDet [16] models with competitive accuracy.



Figure 3. Pose candidate visualizations for both fencers. Selected fencers are highlighted in green.

4.3. Feature engineering

The second stage derives features from pose sequences. Raw joints are informative, but engineered features capture temporal and geometric structure that joints alone do not. We express all skeletons in a canonical left-facing coordinate system: if the active fencer is originally on the right, their 2D joint coordinates are mirrored horizontally about

the frame’s vertical midline. This matches the labeling convention in Section 3.1.

From the 17 available joints we discard five head joints, leaving 12 body joints. To remove background dependence, we compute a scale- and translation-invariant representation by centering each frame at the pelvis and normalizing by average torso length:

$$\tilde{\mathbf{P}}_{i,t} = \frac{\mathbf{P}_{i,t} - \frac{1}{2}(\mathbf{P}_{\text{Lhip},t} + \mathbf{P}_{\text{Rhip},t})}{\frac{1}{2}(\|\mathbf{P}_{\text{Lsh},t} - \mathbf{P}_{\text{Lhip},t}\| + \|\mathbf{P}_{\text{Rsh},t} - \mathbf{P}_{\text{Rhip},t}\|)},$$

where $\mathbf{p}_{i,t} \in \mathbb{R}^2$ is the (x, y) position of joint i at frame t .

From these normalized joints, we derive:

- **Pairwise distances** $d_{ab,t} = \|\tilde{\mathbf{p}}_{a,t} - \tilde{\mathbf{p}}_{b,t}\|$ for hand-to-hand, foot-to-foot, and shoulder/hip widths.
- **Joint angles** at elbows and knees:

$$\theta_{abc,t} = \arccos \frac{(\tilde{\mathbf{p}}_{a,t} - \tilde{\mathbf{p}}_{b,t}) \cdot (\tilde{\mathbf{p}}_{c,t} - \tilde{\mathbf{p}}_{b,t})}{\|\tilde{\mathbf{p}}_{a,t} - \tilde{\mathbf{p}}_{b,t}\| \|\tilde{\mathbf{p}}_{c,t} - \tilde{\mathbf{p}}_{b,t}\|}.$$

- **Torso orientation** as sin and cos of the angle between shoulder and hip centers.
- **Arm extension** as magnitude and normalized direction of shoulder–wrist vectors.
- **Center of mass (CoM)** as the average of all valid joints. To capture dynamics, we include temporal derivatives:

$$\mathbf{v}_{i,t} = \tilde{\mathbf{p}}_{i,t} - \tilde{\mathbf{p}}_{i,t-1}, \quad \mathbf{a}_{i,t} = \mathbf{v}_{i,t} - \mathbf{v}_{i,t-1},$$

for all normalized joints and the CoM.

Each frame is represented by a 101-dimensional vector: 24 joint coordinates, 2 CoM features, 11 distances, 4 angles, 2 torso orientation features, 6 arm-extension features, 24 velocities, 24 accelerations, and 4 CoM velocity/acceleration features. These descriptors serve as input tokens to FERA-MDT.

4.4. FERA-MDT

FERA-MDT is an encoder-only Transformer for multi-label move and blade recognition.

Architecture. Each input frame has 101 features (Sec. 4.3), projected to a 128-dimensional embedding. The model has three encoder layers, each with eight attention heads and a feed-forward dimension of 512, with dropout of 0.1. Temporal aggregation uses masked mean pooling to handle variable-length sequences.

Positional encoding and attention. Temporal structure is preserved through sinusoidal encodings:

$$\begin{aligned} PE_{(pos,2i)} &= \sin\left(\frac{pos}{10000^{2i/d}}\right), \\ PE_{(pos,2i+1)} &= \cos\left(\frac{pos}{10000^{2i/d}}\right). \end{aligned} \quad (1)$$

Multi-head self-attention is applied as

$$\text{Attention}(Q, K, V) = \text{softmax}\left(\frac{QK^\top}{\sqrt{d_k}} + M\right)V,$$

with key-padding mask M to exclude padded tokens.

Output and loss functions. The final layer is a linear classifier (128 \rightarrow 17). The first 12 outputs correspond to moves (multi-label, weighted binary cross-entropy), and the last 5 to blade positions (single-label, softmax cross-entropy). Move loss is

$$L_{\text{move}} = -\frac{1}{N} \sum_i w_i \left[y_i \log \sigma(z_i) + (1 - y_i) \log (1 - \sigma(z_i)) \right], \quad (2)$$

with weights w_i from inverse class frequency. Blade loss is

$$L_{\text{blade}} = -\sum_{c=1}^5 y_c \log \text{softmax}(z)_c.$$

The combined loss is

$$L = L_{\text{move}} + 0.677 L_{\text{blade}},$$

where the blade weight (0.677) was tuned via Optuna to balance gradients and label counts.

Training configuration. Training uses AdamW [15] with learning rate 10^{-3} , weight decay 10^{-4} , and betas (0.9, 0.999). The schedule is 3-epoch warmup, 5-epoch flat, then cosine annealing [14]. Gradients are clipped at $\|g\|_2 \leq 0.5$; batch size is 24. Evaluation uses 5-fold cross-validation with an 80/10/10 split. All experiments are implemented in PyTorch [19].

Data augmentation and balancing. Augmentation is applied after splitting. Methods include temporal jitter ($\Delta t \sim \{-2, \dots, 2\}$), Gaussian noise ($\epsilon \sim \mathcal{N}(0, 0.05^2)$), rotational noise ($\theta \sim U(-0.05, 0.05)$), and scaling ($s \sim U(0.95, 1.05)$). Minority moves are oversampled up to 400 per class, and the majority blade class “6” is downsampled to two-thirds of others.

Hyperparameter selection. Hyperparameters were tuned with Optuna [1]. Across 300 trials, we explored model size, loss weighting, weight decay, and other settings. The top runs were analyzed for recurring patterns, and their best-performing settings were combined into the final model.

4.5. Dynamic temporal windowing

During training and cross-validation, FERA-MDT is optimized on trimmed single-fencer sequences corresponding to labeled exchanges. At deployment, however, we typically receive longer, untrimmed per-fencer pose tracks extracted from bout footage, and the model must decide both how many frames to group into an action and which labels to assign. Fencing actions vary substantially in duration: half-steps may last 4–6 frames, while lunges or compound blade actions can span 30–40 frames. Using a single static window either truncates long actions or dilutes short ones with irrelevant context. FERA-MDT therefore uses dynamic temporal windowing during inference.

Given a per-fencer pose sequence $\{x_t\}_{t=1}^T$, where T can range from a short clip to an entire bout segment, we process frames in segments beginning at index s , with initial window $w_0 = 1$. For each window $[s, s + w - 1]$, FERA-MDT produces move logits and a blade-line distribution. If the maximum move confidence is below a threshold τ (per-class thresholds are tuned via validation), the window expands by one frame, $w \leftarrow w + 1$, up to $w_{\max} = 40$. If no confident prediction emerges by w_{\max} , the window is reset to w_0 and the start index advances by one frame, $s \leftarrow s + 1$. For half-steps, the system checks for a subsequent full step before finalizing the label, to avoid over-fragmenting continuous footwork into many very short predictions.

This adaptive strategy allows short actions to be recognized promptly, while longer actions accumulate sufficient context. It reduces boundary errors and improves recognition of compound actions such as step forward + beat, which are often ambiguous when only partial motion is visible. Because s can start at any frame and the window can grow up to w_{\max} , the procedure applies to any sequence length T : the same classifier trained on trimmed segments acts as a local detector over a continuous pose stream. Predicted move intervals across consecutive windows are merged using non-maximum suppression on overlapping time spans, yielding a final per-fencer sequence of moves and blade positions aligned with the clip or bout timeline.

4.6. FERA-LM: Semantic Reasoning Interface

After generating move and blade predictions, the system requires a mechanism to bridge the gap between semantic labels and logical rule application. FERA-LM serves as this interface. Rather than functioning as a standalone referee, FERA-LM is designed to validate the semantic representational power of the detected actions.

Using DeepSeek-R1-Distill-Qwen-14B as the teacher model [7], we generate referee decisions with a structured prompt that (i) lists the relevant foil rules retrieved via a FAISS index [13], (ii) provides the left and right fencer move sequences with blade positions, and (iii) requests a two-part answer: a single-line decision (Left / Right / None)

and a brief explanation referencing the rules and moves. Responses are constrained to be concise and deterministic for consistent outputs [24].

The student model is DistilGPT-2, trained with causal language modeling on the teacher’s outputs [11]. This yields a smaller, cheaper model while retaining decision quality. Both teacher and student are supervised to reproduce the official referee decision derived from the scoreboard.

5. Results

We evaluate FERA via (i) an end-to-end example showing how the full pipeline produces referee decisions, and (ii) quantitative comparisons of FERA-MDT with baseline models, including ablations.

5.1. End-to-end Logic Consistency

We illustrate one clip where the referee ruled that the left fencer held priority. FERA-MDT correctly identifies the actions for both fencers, and FERA-LM produces a decision and explanation that align with the referee’s judgment.

Crucially, this example demonstrates the logical consistency of the decoupled framework. Even if intermediate move detection errors occur (e.g., missing a minor blade beat), the language model can often recover the correct priority flow if the primary attack sequence (Lunge vs. Retreat) is correctly identified. This suggests that the kinematic features captured by FERA-MDT form a sufficient semantic vocabulary for fencing logic.

Rules.

If an attack is initiated but falls short or misses, priority shifts to the other fencer.

Priority is given to the fencer who initiates the attack unless it is interrupted.

Fencing moves:

Left: [80–112] step forward (blade pos. 8); [112–134] step forward + beat (blade pos. 8); [134–146] lunge + hit (blade pos. 6).

Right: [83–110] step backward (blade pos. 6); [110–138] fake (blade pos. 6); [138–148] counterattack + hit (blade pos. 6).

Model output.

Decision: Left

Explanation: The left fencer initiates the attack with a step forward while the right fencer retreats. The left fencer then performs a lunge, hit (134–146) and the right fencer responds with counterattack, hit (138–148). Under the rules, priority remains with the initial attacker and does not transfer to the right fencer.

!!!



(a) Left step forward + beat, right stepping back. (b) Left lunge, right counterattack.

Figure 4. Illustrative frames from the bout corresponding to the described moves.

5.2. Evaluation metrics

We report four classification metrics and three calibration metrics.

Classification.

- Macro-F1 = $\frac{1}{C} \sum_c F1_c$: averages F1 over classes, emphasizing rare moves.
- Weighted-F1 = $\sum_c \frac{n_c}{\sum_j n_j} F1_c$: weights each class by frequency.
- Micro-F1 = $\frac{2 \sum_c TP_c}{2 \sum_c TP_c + \sum_c FP_c + \sum_c FN_c}$: global F1 over all labels.
- Hamming loss = $\frac{1}{NC} \sum_{i=1}^N \sum_{c=1}^C \mathbf{1}[y_{i,c} \neq \hat{y}_{i,c}]$: fraction of misclassified labels; lower is better.

For class c ,

$$P_c = \frac{TP_c}{TP_c + FP_c}, \quad R_c = \frac{TP_c}{TP_c + FN_c}, \quad F1_c = \frac{2P_c R_c}{P_c + R_c}.$$

Calibration.

$$ECE = \sum_{m=1}^M \frac{|B_m|}{N} |\text{acc}(B_m) - \text{conf}(B_m)|,$$

$$MCE = \max_m |\text{acc}(B_m) - \text{conf}(B_m)|,$$

$$\text{Brier} = \frac{1}{NC} \sum_{i=1}^N \sum_{c=1}^C (y_{i,c} - \hat{p}_{i,c})^2.$$

ECE summarizes average calibration quality; MCE highlights worst-case miscalibration; the Brier score combines calibration and sharpness.

5.3. Move detection model comparisons

Table 2 compares FERA-MDT with three baselines. FERA-MDT consistently outperforms all baselines on Macro-F1 and Hamming loss, indicating stronger performance on both common and rare moves. BiLSTM comes closest, as recurrent architectures capture short-term motion well, but the encoder-only structure of FERA-MDT appears better suited to the multi-label, long-range dependencies in our setting. The baseline Transformer underperforms slightly despite similar depth, suggesting that pooling and loss weighting matter. TCN achieves the highest Weighted-F1, reflecting a bias toward dominant classes such as step forward and hit, which is undesirable for refereeing, where rare actions also matter.

Table 3 reports calibration metrics. BiLSTM and the baseline Transformer are substantially worse calibrated than

FERA-MDT and TCN. Between the latter two, TCN attains lower ECE and MCE but a higher Hamming loss, indicating that its apparent calibration partly reflects overspecialization on frequent classes. FERA-MDT offers a better trade-off between calibration and rare-class recognition.

Model	Macro-F1 \uparrow	Micro-F1 \uparrow	Weighted-F1 \uparrow	Hamming \downarrow
FERA-MDT	0.549	0.543	0.558	0.158
BiLSTM [20]	0.537	0.531	0.550	0.166
Baseline Transformer	0.533	0.524	0.546	0.170
Temporal CNN (TCN) [2]	0.520	0.519	0.569	0.184

Table 2. Classification performance averaged across 5 folds.

Model	ECE \downarrow	MCE \downarrow	Brier \downarrow
FERA-MDT	0.152	0.458	0.135
BiLSTM	0.187	0.512	0.146
Baseline Transformer	0.191	0.498	0.143
Temporal CNN (TCN)	0.110	0.446	0.140

Table 3. Calibration metrics averaged across 5 folds.

Overall, FERA-MDT attains the best combination of macro-F1, Hamming loss, and Brier score among the tested models, making it the strongest candidate for downstream referee assistance.

5.4. Co-occurrence analysis

Referee decisions depend on combinations of actions, so we assess whether models reproduce the ground-truth co-occurrence structure. Figures 5–8 show co-occurrence mappings. The left matrix in each plot shows ground-truth labels, and the right shows model predictions. FERA-MDT produces mappings that most closely mirror the ground truth; baselines tend to over-activate frequent moves and underrepresent rarer ones.

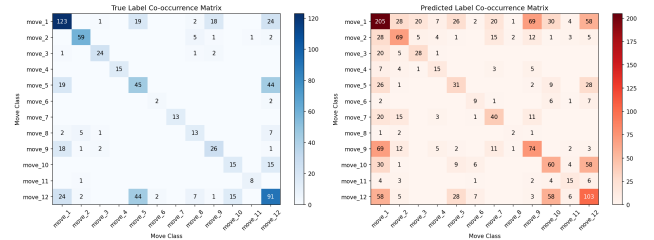


Figure 5. Co-occurrence mapping (Fold 5) for FERA-MDT.

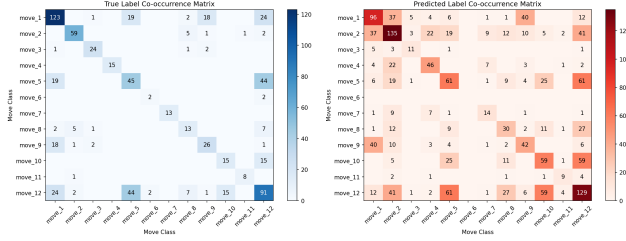


Figure 6. Co-occurrence mapping (Fold 5) for BiLSTM.

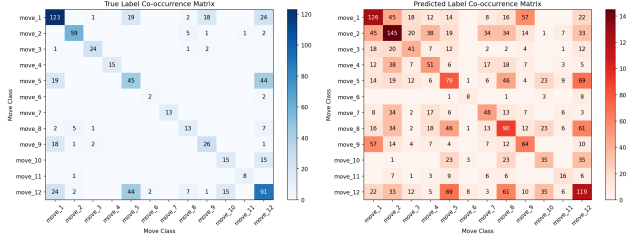


Figure 7. Co-occurrence mapping (Fold 5) for the baseline Transformer.

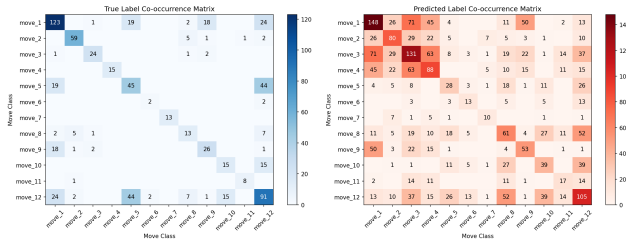


Figure 8. Co-occurrence mapping (Fold 5) for the Temporal CNN (TCN).

5.5. Ablations

We perform ablations on FERA-MDT while keeping all other settings fixed. We report classification (Macro-F1) and calibration (ECE, MCE, Brier) metrics averaged over five folds [3, 8].

Table 4 summarizes the results. The full configuration achieves the highest Macro-F1 (0.549) with strong calibration (ECE = 0.152, MCE = 0.458, Brier = 0.135). Removing per-class thresholds reduces Macro-F1 to 0.511, confirming their importance. Using only the 12 normalized joints (24D) yields Macro-F1 of 0.534, showing that engineered features improve performance but are not strictly required; calibration, however, deteriorates, indicating that features primarily enhance reliability.

Augmentation strategies provide complementary gains. Individually, noise-only, temporal-only, and feature-specific augmentations yield Macro-F1 scores of 0.542, 0.525, and 0.537, respectively. Combining all strategies produces the

best robustness and top score (0.549). Figures 9 and 10 illustrate how single augmentations can be unstable across folds, underscoring the need for combined augmentation and calibration.

Per-class temperature scaling improves calibration without changing F1, and down-weighting blade loss slightly benefits both calibration and classification.

Overall, FERA-MDT’s complete design—feature engineering, diverse augmentation, calibrated thresholds, and tailored loss weighting—is necessary to achieve both strong classification and reliable confidence estimates.

Variant	Macro-F1 ↑	ECE ↓	MCE ↓	Brier ↓
All Features	0.549	0.152	0.458	0.135
No per-class thresholds	0.511	0.140	0.460	0.137
Raw joints (24D, no features)	0.534	0.184	0.515	0.149
Noise-only augmentation	0.542	0.175	0.467	0.141
Temporal augmentation only	0.525	0.200	0.535	0.164
Feature-specific augmentation only	0.537	0.154	0.487	0.144
No augmentation	0.541	0.176	0.545	0.150
No per-class temperature scaling	0.549	0.178	0.493	0.142
Equal loss weights (move = blade)	0.544	0.179	0.499	0.146

Table 4. Ablations: Macro-F1 and calibration metrics (average over 5 folds).

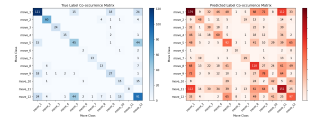


Figure 9. Feature-specific augmentation only (Fold 2, poor performance).

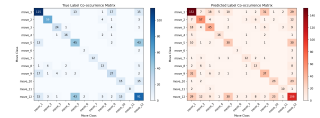


Figure 10. Feature-specific augmentation only (Fold 3, strong performance).

6. Limitations and Future Work

The primary constraint is data. With no public datasets containing extensive move annotations, we relied on manual labeling. Performance improved steadily as the dataset grew: with ~1,000 annotated segments, F1 plateaued near 0.40, while doubling to 2,000 segments raised F1 to 0.549. Long-tail actions remain a bottleneck; expanding the dataset, especially for rare moves, should further improve accuracy.

FERA also depends on generic pose detectors that do not support blade detection. A blade-specific extractor would allow FERA-MDT to incorporate precise blade positions and more reliable contact cues. At the reasoning stage, FERA-LM inherits FERA-MDT’s errors, since teacher generation and student distillation are both conditioned on predicted moves. Improving move detection should therefore also improve language-model decisions.

Evaluating language-based reasoning is another open issue. Our dataset includes final referee decisions (via synchronized scoreboard changes), and both teacher and stu-

dent are supervised to reproduce these outcomes. However, we cannot disentangle FERA-LM’s contribution from upstream recognition errors, and we lack ground-truth textual justifications from referees. Broadcast footage does not provide access to the referee’s phrasing or intermediate reasoning, so we cannot directly measure explanation quality. The end-to-end example in Section 5 should thus be viewed as a qualitative demonstration. A fuller study would collect structured referee judgments or explanations and evaluate both decision accuracy and explanation usefulness, as in recent VARS work.

Generalization also remains a challenge. Our dataset consists exclusively of professional fencers, often recorded from elevated camera angles, which may limit adaptability to beginners and to different viewpoints. Future work may incorporate 3D joint extraction to mitigate camera-angle sensitivity and extend testing to broader fencer populations.

Finally, we do not use athlete-disjoint splits, as we lack metadata to link clips to individual fencers. While our dataset spans roughly 130 competitors, some overfitting to individuals is still possible.

Overall, these limitations suggest a roadmap: larger and more diverse datasets, explicit blade detection, quantitative evaluation of language-based reasoning, improved distillation from cleaner labels, and greater attention to generalization. Addressing these factors will enable more dependable referee assistance and broader coaching applications.

7. Conclusion

Modern foil refereeing is entirely manual; only the hit lights are automated. No systems currently assist or validate human decisions in this setting. Prior work on fencing move recognition has been limited to small subsets of footwork actions and often uses specialized sensors.

FERA is a first prototype referee assistant that operates directly from monocular video. We present a pose-based pipeline for recognizing multi-label moves and blade positions for individual fencers, a new dataset with frame-level annotations from real competition footage, and a decoupled system that integrates motion recognition with rule-grounded reasoning. FERA-MDT’s macro-F1 of 0.549 highlights the difficulty of this setting but also demonstrates the feasibility of Transformer-based motion understanding under real-world conditions. By aggregating recognized actions and blade positions from both sides of the piste, and by running the same model over continuous pose streams using dynamic temporal windowing, the same machinery can support both referee assistance and coaching or tactical analysis. We will release the FERA-Dataset annotations, derived pose features, and baseline code to encourage further work on pose-based motion understanding and AI-assisted sports officiating.

References

- [1] Takuya Akiba, Shotaro Sano, Toshihiko Yanase, Takeru Ohta, and Masanori Koyama. Optuna: A next-generation hyperparameter optimization framework. In *Proceedings of the 25th ACM SIGKDD International Conference on Knowledge Discovery & Data Mining*, page 2623–2631, New York, NY, USA, 2019. Association for Computing Machinery.
- [2] Shaojie Bai, J. Zico Kolter, and Vladlen Koltun. An empirical evaluation of generic convolutional and recurrent networks for sequence modeling, 2018.
- [3] Glenn W. Brier. Verification of forecasts expressed in terms of probability. *Monthly Weather Review*, 78(1):1–3, 1950.
- [4] Zhe Cao, Gines Hidalgo, Tomas Simon, Shih-En Wei, and Yaser Sheikh. Openpose: Realtime multi-person 2d pose estimation using part affinity fields. *IEEE Transactions on Pattern Analysis and Machine Intelligence*, 43(1):172–186, 2021.
- [5] Kai Chen, Jiaqi Wang, Jiangmiao Pang, Yuhang Cao, Yu Xiong, Xiaoxiao Li, Shuyang Sun, Wansen Feng, Ziwei Liu, Jiarui Xu, et al. Mmdetection: Open MMLab detection toolbox and benchmark. *arXiv preprint arXiv:1906.07155*, 2019.
- [6] Anthony Cioppa, Mehdi Chouiten, Pranav Chaudhari, Marco Ciaperoni, Mario Mezzani, Johannes T. Holz, Junqing Lv, Mitra Baratchi, Carlos H. M. De Souza, Hersh Shukla, Adriaan S. Hendricks, Silvio Giancola, Bernard Ghanem, Jan C. van Gemert, Cees G. M. Snoek, Hugo Mercier, Adrien Deliege, and Marc Van Droogenbroeck. Soccernet 2024 challenges results. In *Proceedings of the IEEE/CVF Conference on Computer Vision and Pattern Recognition (CVPR) Workshops*, pages 3256–3266, 2024.
- [7] DeepSeek-AI. Deepseek-r1-distill-qwen-14b (model card). <https://huggingface.co/deepseek-ai/DeepSeek-R1-Distill-Qwen-14B>, 2025. accessed: 2025-09-08.
- [8] Chuan Guo, Geoff Pleiss, Yu Sun, and Kilian Q. Weinberger. On calibration of modern neural networks. In *Proceedings of the 34th International Conference on Machine Learning*, pages 1321–1330. PMLR, 2017.
- [9] Jan Held, Anthony Cioppa, Hani Itani, Bernard Ghanem, and Marc Van Droogenbroeck. VARS: Video assistant referee system for automated soccer decision making from multiple views. In *Proceedings of the IEEE/CVF Conference on Computer Vision and Pattern Recognition (CVPR) Workshops*, pages 3179–3188, 2023.
- [10] Jan Held, Hani Itani, Anthony Cioppa, Silvio Giancola, Bernard Ghanem, and Marc Van Droogenbroeck. X-VARS: Introducing explainability in football refereeing with multi-modal large language model. In *Proceedings of the IEEE/CVF Conference on Computer Vision and Pattern Recognition (CVPR) Workshops*, pages 3267–3279, 2024.
- [11] Hugging Face. Distilgpt-2 (model card). <https://huggingface.co/distilbert/distilgpt2>, 2024. accessed: 2025-09-08.
- [12] Tao Jiang, Peng Lu, Li Zhang, Ningsheng Ma, Rui Han, Chengqi Lyu, Yining Li, and Kai Chen. Rtmpose: Real-time multi-person pose estimation based on mmpose, 2023.

- [13] Jeff Johnson, Matthijs Douze, and Hervé Jégou. Billion-scale similarity search with gpus. *IEEE Transactions on Big Data*, 7(3):535–547, 2021.
- [14] Ilya Loshchilov and Frank Hutter. SGDR: Stochastic gradient descent with warm restarts. In *International Conference on Learning Representations*, 2017.
- [15] Ilya Loshchilov and Frank Hutter. Decoupled weight decay regularization. In *International Conference on Learning Representations*, 2019.
- [16] Chengqi Lyu, Wenwei Zhang, Haiyan Huang, Yue Zhou, Yudong Wang, Yanyi Liu, Shilong Zhang, and Kai Chen. Rtmddet: An empirical study of designing real-time object detectors, 2022.
- [17] Filip Malawski. Fencing footwork dataset (ffd). <https://home.agh.edu.pl/~fmal/ffd/>, 2016. accessed: 2025-09-08.
- [18] OpenMMLab. Mmpose: OpenMMLab pose estimation toolbox and benchmark. <https://github.com/open-mmlab/mmpose>, 2024. accessed: 2025-09-08.
- [19] Adam Paszke, Sam Gross, Francisco Massa, Adam Lerer, James Bradbury, Gregory Chanan, Trevor Killeen, Zeming Lin, Natalia Gimelshein, Luca Antiga, et al. PyTorch: An imperative style, high-performance deep learning library. In *Advances in Neural Information Processing Systems (NeurIPS)*, 2019.
- [20] M. Schuster and K.K. Paliwal. Bidirectional recurrent neural networks. *IEEE Transactions on Signal Processing*, 45(11):2673–2681, 1997.
- [21] TryoLabs. Norfair documentation. <https://tryolabs.github.io/norfair/2.2/reference/>, 2023. accessed: 2025-09-08.
- [22] TryoLabs. Norfair: Lightweight python library for real-time multi-object tracking. <https://github.com/tryolabs/norfair>, 2023. accessed: 2025-09-08.
- [23] Nicolai Wojke, Alex Bewley, and Dietrich Paulus. Simple online and realtime tracking with a deep association metric. In *2017 IEEE International Conference on Image Processing (ICIP)*, pages 3645–3649, 2017.
- [24] Thomas Wolf, Lysandre Debut, Victor Sanh, Julien Chaumond, Clément Delangue, Anthony Moi, Pierric Cistac, Tim Rault, Rémi Louf, Morgan Funtowicz, et al. Transformers: State-of-the-art natural language processing. In *Proceedings of the 2020 Conference on Empirical Methods in Natural Language Processing: System Demonstrations (EMNLP Demos)*, pages 38–45, 2020.
- [25] Bin Xiao, Haiping Wu, and Yichen Wei. Simple baselines for human pose estimation and tracking. In *Proceedings of the European Conference on Computer Vision (ECCV)*, pages 466–481, 2018.
- [26] Yufei Xu, Jing Zhang, Qiming Zhang, and Dacheng Tao. Vit-pose: Simple vision transformer baselines for human pose estimation, 2022.
- [27] Yifu Zhang, Peng Sun, Yi Jiang, Dongdong Yu, Xinze Weng, Zhaoqi Yuan, Ping Luo, Wen Liu, and Xiaogang Wang. ByteTrack: Multi-object tracking by associating every detection box. In *Proceedings of the European Conference on Computer Vision (ECCV)*, 2022.
- [28] Kevin Zhu, Alexander Wong, and John McPhee. Fencenet: Fine-grained footwork recognition in fencing. In *CVPR Workshops*, 2022.